Mon. Not. R. astr. Soc. (1989) **237**, 799–826 and *Microfiche* MN 237/3

The dynamics of rich clusters – II. Luminosity functions

Matthew Colless *Department of Physics, University of Durham, Science Laboratories, South Road, Durham DH1 3LE*

Accepted 1988 October10. Received 1988 August 17; in original form 1988 April 27

Summary. This is the second paper in an observational survey of the dynamical properties of 14 rich clusters of galaxies. Paper I in the series outlined the strategy of the survey and presented the radial velocities and stellar velocity dispersions obtained from multiplex spectroscopy of the clusters. This paper presents photographic photometry for the clusters and examines their luminosity functions (LFs).

The individual cluster LFs are found to be well fitted by Schechter functions with $\alpha \equiv -1.25$. The mean characteristic magnitude M^* is -20.12 in B_J ($H_0 = 100$ km s^{-1}), in good agreement with previous determinations. The composite LF formed from all 14 clusters is best fitted by a Schechter function with $M^* = -20.04$ and $\alpha = -1.21$. Various statistical tests provide no evidence that, over the range M^*-1 to M^*+2 examined here, individual cluster LFs are not all drawn from a universal cluster LF having approximately Schechter form and parameters $M^* \approx -20.1$ and $\alpha \approx -1.25$. Simulations show, however, that the small number of galaxies in the bright end of cluster LFs limits the statistical discrimination between differing LFs to a level greater than the smallest differences of physical interest.

Comparisons of composite LFs formed by grouping rich and poor clusters, and clusters of Bautz–Morgan (B–M) types I and I–II and B–M type III, reveal no variation of cluster LFs with either richness or B–M type. A similar comparison, however, marginally suggests that the composite LF of the high velocity dispersion clusters has a fainter M^* than that of the low velocity dispersion clusters. No evidence for mass segregation in the form of LF differences between the centres and peripheries of the clusters is found. Simulations to assess the power of the statistical tests imply that variations of more than 0.4 mag in M^* or 0.15 in α are ruled out by these comparisons. However, the reliable detection of smaller variations, such as those of the size expected due to differing morphological mixes, will require an increase by a factor of at least 4 in the size of the sample of cluster LFs.

1 Introduction

The study of cluster luminosity functions (LFs) has had two themes running concurrently throughout. One, emphasized particularly in the earlier studies (see the review by Abell 1975), lays stress on the similarities between cluster LFs and between cluster LFs and the field LF, motivated by the uses to which a 'universal' LF could be put – notably as a standard candle in cosmology. The second theme is the search for differences between the various LFs (see, for example, Dressler 1978) which might act as indicators for differences in galaxy formation due to differing environments, or for modifications of a common primeval LF by dynamical processes occurring during or after the collapse of clusters.

Since the form of the cluster and field LFs is intimately related to the mechanisms of galaxy formation, the comparison of cluster LFs with the field LF, and with each other, should (in principle at least) illuminate some of the dynamical interactions occurring in clusters since galaxy formation, and/or the differences between galaxy formation in clusters and the field. At present, too little is known theoretically for the observed form of the LF to be usefully related to galaxy formation. However, several recent studies (e.g. Miller 1983; Malamuth & Richstone 1984; Merritt 1983, 1984, 1985) have made simple predictions which relate various dynamical processes occurring in clusters after galaxy formation to the form of the cluster LFs.

The question then arises of whether individual cluster LFs are indeed sample populations drawn from a single distribution ('strong' universality of the LF), or whether there are real variations, the combined LF merely approaching the universal LF for large samples of clusters ('weak' universality of the LF). The largest previous studies of cluster LFs, those of Dressler (1978) and Lugger (1986), reach opposite conclusions on this point. Dressler finds that 'although [the LFs] are similar in general appearance, variations exist which are significantly greater than would be expected for statistical fluctuations of a universal function'. However, Lugger finds that 'the cluster LFs studied form a fairly homogeneous sample' and that there are no significant correlations between the form of the clusters' LFs and their morphology.

These studies and others (e.g. those of Oemler 1974; Godwin 1976; and Schechter 1976) show clearly that clusters do have generally similar forms for their LFs. Moreover, the very close agreement of the parameters obtained in the mean for samples of ~ 10 clusters by these authors implies that, if cluster LFs are significantly different, statistical convergence to a universal LF in the mean is extremely rapid. Thus it would seem most natural to adopt 'strong' universality as our null hypothesis and seek first to disprove it.

There are two basic approaches to this goal. The first is to compare cluster LFs with each other or with an assumed universal LF, either directly by statistical tests measuring the likelihood that two samples are drawn from the same distribution (or that an observed distribution is drawn from a hypothetical parent), or indirectly by comparing the parameters of functional fits to the LFs. This approach faces the difficulty that the number of galaxies in any individual cluster LF is relatively small for the purpose of statistically detecting variations of the sizes expected from simulations of cluster evolution. The second approach attempts to surmount this problem by seeking variations not on a cluster-by-cluster basis but for sets of clusters defined (independently of their LFs under the null hypothesis) on grounds which it might be suspected should lead to intrinsic LF differences (such as mix of galaxy types or richness).

This paper presents photographic photometry for the galaxies in 14 rich clusters and examines their luminosity functions following the strategy described above. A previous paper (Colless & Hewett 1987 – Paper I) presented radial velocities and stellar velocity dispersions for about 40 galaxies in each of these 14 clusters. Future papers will examine the spatial structure, velocity distributions and dynamics of the clusters, in order to provide a general picture of the dynamics in clusters covering a broad range in richness and morphological type.

2 Data

2.1 THE SAMPLE OF CLUSTERS

The 14 clusters comprising this study are all drawn from a preliminary version of Abell & Corwin's southern cluster survey (hereafter SCS), supplied by H. G. Corwin (private communication). A general description of the SCS is given by Abell & Corwin (1983). The extent of the SCS is unique in the southern hemisphere, and the high quality of the UK Schmidt Telescope IIIa-J sky survey plate material used in its compilation makes it probably the most complete cluster catalogue in existence. As far as possible, the SCS mimics the Abell catalogue for northern clusters (Abell 1958).

The clusters studied here were drawn, on the basis of availability of plate material and observational expedience, from a complete sample of clusters having:

(i) redshifts, estimated from m_{10} (the visual magnitude of the tenth-brightest cluster galaxy), in the range $0.03 \le z \le 0.1$;

(ii) an Abell richness count (the number of galaxies within an Abell radius, approximately 1.5 h^{-1}Mpc,* having magnitudes in the range $m_3 \le m \le m_3 + 2$) of ≥ 70 galaxies;

(iii) galactic latitude $|b| > 30°$.

The sole exception is the additional cluster AC1, observed during an initial trial observing run. This has a richness count of 59.

The cluster sample is listed in Table 1. Positions and richnesses are from the SCS. The cluster redshifts are from Paper I. The Abell richness count, N_A, and richness class, R_A, are derived from Abell & Corwin's raw counts within an Abell radius, by first correcting for the expected number of field galaxies (tabulated in the SCS using the luminosity function of Rainey 1977). The calibration formula

$$N_A = N_C - 80 + 18 \ln(N_C - 34) \quad (1)$$

Table 1. The cluster sample.

(1) Cluster ID	(2) R.A. (1950)	(3) Dec. (1950)	(4) z	(5) N_A	(6) R_A	(7) Other ID[a]
C02	00 00.7	-36 14	0.04925	81	2	
C03	00 03.6	-35 00	0.11598	208	4	
C19	03 27.4	-55 53	0.08588	72	1	
C20	03 29.2	-52 47	0.05938	131	3	DC0329–52
C21	03 43.6	-24 26	0.10560	92	2	A458
AC1	04 08.6	-59 43	0.05489	59	1	
C30	05 17.2	-58 36	0.09655	81	2	
C31	05 38.8	-43 25	0.08450	85	2	
C37	20 38.5	-35 25	0.08967	108	2	
C39	20 48.5	-52 08	0.04818	82	2	DC2048–52
C52	22 14.8	-35 58	0.14922	138	3	
C64	23 05.9	-20 11	0.08291	104	2	A2538
C65	23 09.7	-21 48	0.11094	114	2	A2554
C67	23 49.5	-34 40	0.05846	72	1	

[a] Abell (1958 or Dressler (1980a) ID. See also table 5 of Paper I.

* Here and throughout, $H_0 = 100\ h$ km s^{-1}.

is then applied to convert the field-corrected count, N_C, to Abell's (1958) richness count, N_A. This empirical relation is given in the SCS and is based on the comparison of data for about 120 Abell clusters in the overlap of the SCS with the original Abell catalogue.

2.2 PLATE MATERIAL

The plate material on which the new cluster photometry is based is listed in Table 2. All plates were taken as part of the J Southern Sky Survey (SSS) by the UK Schmidt Telescope (UKST) at Siding Spring, Australia. A full description of the survey can be found in the UKST Handbook and references therein.

The pass-band for these plates is defined by the combination of the IIIa-J emulsion response and a GG395 filter, and will be denoted B_J. The transformation from the standard B and V photometric pass-bands is

$$B_J = B - (0.28 \pm 0.04)(B - V) \tag{2}$$

over the range $-0.1 \leq (B-V) \leq 1.6$ (Blair & Gilmore 1982).

Column 2 of Table 2 gives the SSS field numbers to which the plates correspond. Given in parentheses are overlap SSS fields in which the cluster also falls. All the plates are copies, except for J6392, and all are of survey standard (grades 1–3; see the UKST Handbook) over the region of the cluster, although emulsion flaws or other defects elsewhere on the plate mean that some are not included in the SSS.

Survey-grade plates and their copies are required to meet stringent requirements for resolution (image size), image shape, and exposure depth, which are described in Cannon *et al.* (1978). This quality control ensures a high degree of uniformity in the survey-grade plates, as is evidenced by the calibrating photometry discussed in Section 2.4.

Table 2. Plate material.

(1) Cluster ID	(2) SSS[a] field	(3) Plate	(4) Exposure[b] time (*min*)	(5) B_J limit
C02	349	J6145	65	18.9
C03	349	J6145	65	19.7
C19	155	J6392	65	18.8
C20	155	J6392	65	18.5
C21	482	J3620	75	20.0
AC1	118(117)	J8358	65	19.4
C30	119	J3787	75	20.0
C31	253	J2715	70	20.0
C37	401	J6109	60	20.1
C39	235(187)	J3389	70	19.3
C52	405	J6231	65	20.3
C64	604	J3654	70	20.1
C65	604	J3654	70	20.2
C67	349(408)	J6145	65	19.2

[a]Overlap SSS fields in which the cluster also lies are given in parentheses.
[b]Exposure times are from the UKST plate catalogue.

2.3 PHOTOGRAPHIC PHOTOMETRY WITH THE APM

The Automated Photographic Measuring System (APM) at the Institute of Astronomy in Cambridge consists of a laser scanning microdensitometer, permitting high-speed scanning with low measurement noise, and a series of specialized computers for on-line processing of the data (Kibblewhite *et al.* 1983).

All measurements are performed in two passes. The first of these allows an estimate of the sky background to be made. The plate is partitioned into regions each of 64×64 pixels (with 1 pixel $= 8\ \mu$m $= 0.537$ arcsec). The interpolated mode of the intensities of these pixels is taken as an initial estimate of the sky background for that region. The entire 2D array of initial background estimates covering the whole plate is then passed through a non-linear filter which detects and corrects background values contaminated by the presence of resolved images and smooths the array to give the final map of background estimates for the plate.

On the second pass over the plate, a threshold is defined as a fixed additive isophote above the local sky background, in this case twice the rms noise in the measured sky value, which for UKST J copies corresponds to between 8 and 11 per cent of the sky surface brightness, or about 24.5 mag arcsec^{-2}. Images are detected as regions of greater than a fixed number of connected pixels (here 25) lying above this threshold. Image parameters (integrated isophotal intensity, position, second-order moments, peak intensity and areal profile) are computed on-line before being stored on magnetic tape for further off-line processing.

The 12-bit measured transmission (T) of each pixel in the scan is converted to a 10-bit density (D) using a look-up table corresponding to

$$D = \frac{1024}{2.5} \log\left(\frac{4096}{T}\right), \tag{3}$$

giving a maximum density range of 2.5. The APM isophotal intensity measure I_{APM} is the sum of the sky-subtracted densities of the pixels which make up an image (as I is approximately linear with D over a range of about 2 in density above the plate fog level). APM 'magnitudes' are defined as $2.5 \log I_{\mathrm{APM}}$. The x–y position of the image is computed as the density-weighted mean of these pixels. Together with the peak intensity and shape parameters (second-order moments and areal profile), these provide virtually all the useful information contained in the fainter images. Because the threshold is a fixed additive level above local background, the image parameters are dependent on optical vignetting and sensitivity variations on the plate but are independent of real-sky variations, changes in fog level or other additive effects.

The APM positions have a relative accuracy for faint stellar images of about 0.1 arcsec and about 0.3 arcsec for extended objects such as galaxies. Absolute right ascensions and declinations, obtained by fitting a six-parameter transform plus radial correction to the Perth 70 catalogue positions of the 20 brightest stars on the plate, are typically accurate to 1.0 arcsec. Further details of the operation and performance of the APM can be found in the APM Handbook and Irwin & Trimble (1984).

2.4 PHOTOMETRIC CALIBRATION

Photometric calibration for 11 of the 14 clusters comes from CCD observations made on the 1.5-m telescope at Cerro Tololo InterAmerican Observatory (CTIO) during the nights of 1987 July 29 and 30. The CCD used was CTIO RCA #5 without preflashing. One or two fields (each 2.9×4.6 arcmin) close to the centre of each cluster were observed, with two exposures in both B and V taken for each field. The integration times for B exposures were 600 s and for V exposures 300 s.

Eleven Landolt (1983) photometric standard stars were observed in B and V during the first night and 10 during the second, with two exposures taken in each colour. Bias subtraction, dark-current subtraction and flat-fielding of all images was performed with the Image Reduction and Analysis Facility (IRAF; described in the IRAF User Handbook and Tody 1986). The photometric standards were reduced using the KPNO Mountain Photometry Code (MPC) stellar photometry software (Adams *et al.* 1980) assuming standard extinctions. The standard deviations in the derived B and V photometric constants over the set of standard stars are 0.04 and 0.01 mag, respectively. The differences in the standards between the first and second nights were less than 0.01 mag in each band.

Isophotal magnitudes for the galaxies in each CCD field whose images were uncontaminated by nearby objects were derived using the GASP surface photometry software written by Mike Cawson at the Institute of Astronomy, Cambridge. Integrated B and V magnitudes were obtained within the $B = 26.0$ mag arcsec^{-2} isophote and converted to B_J using equation (2). Photometric calibrations of the photographic magnitudes for each cluster were then found by performing a linear regression between the isophotal CCD magnitudes and the APM instrumental magnitudes for these galaxies. The standard deviations about these regressions were all <0.2 mag. The dispersion in the slopes of the regressions was 6 per cent.

This remarkable consistency of the APM magnitudes from plate to plate is illustrated in Fig. 1, which shows isophotal CCD B_J magnitude versus APM instrumental magnitude for each galaxy in every field, undifferentiated. The standard deviation about the mean of the individual cluster calibrations (the line in the figure) is 0.25 mag. We therefore adopt this mean calibration for the three clusters without CCD calibrations (AC1, C30, C31), expecting typical systematic errors of ± 6 per cent in the slope of the calibration and ± 0.15 mag in the zero-point.

2.5 COMPARISON WITH PUBLISHED PHOTOMETRY

Carter (1980) presents multiband photometry for galaxies in the field of C03, obtained from PDS measurements of AAT and UKST plates. The photographic pass-band of the blue

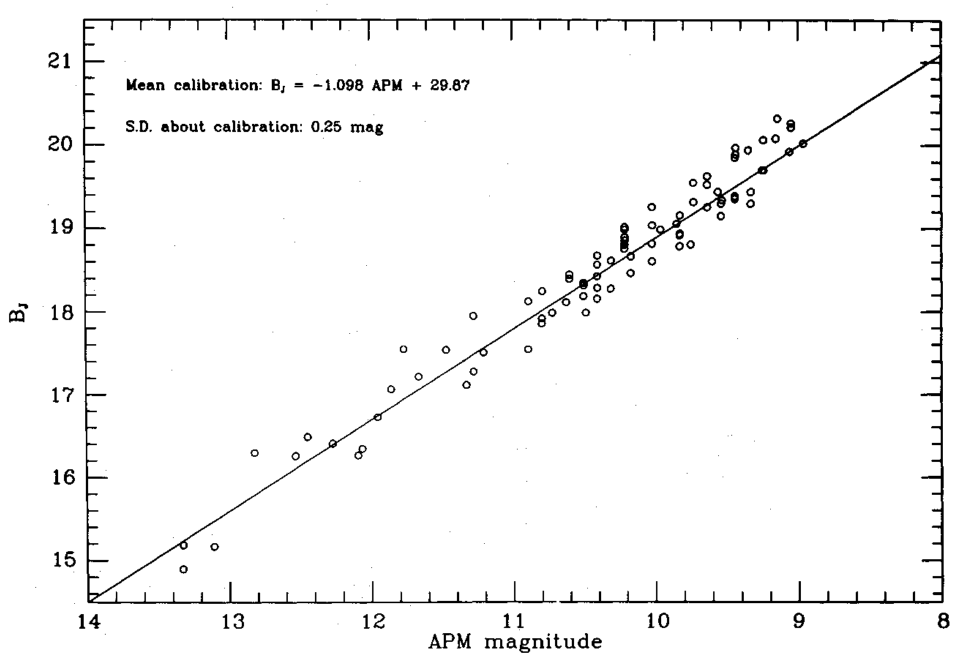

Figure 1. Isophotal (26 mag arcsec^{-2} B_J CCD magnitudes versus APM instrumental magnitudes for each calibration galaxy in every cluster field. The solid line is the mean of the calibrations for the individual clusters. The standard deviation of the points about the line is 0.25 mag.

Schmidt plate was defined by the combination of IIIa-J emulsion and a GG395 filter (i.e. B_J), while that of the AAT plate was defined by the combination of IIIa-J emulsion and a GG385 filter (which Carter labels b). The blue magnitudes tabulated by Carter are taken from the AAT plate and are measured within the 27 mag arcsec^{-2} isophote.

The zero-point (extinction-reduced sky brightness) was derived for the Schmidt plate by comparison with B photoelectric photometry of the galaxies NGC 7793 ($B-V=0.6$) and PKS 2354 – 35 ($B-V=1.1$) by Green & Dixon (1978). Carter's magnitude system b_C is thus $b_C \approx B-0.23(B-V)+0.20$, where we have used the transformation $b=B-0.23(B-V)$ given by Kron (1980). The constant in this expression is obtained from the condition that $b_C=B$ for $B-V=0.85$, the mean $B-V$ of the two standard galaxies. By equation (2), we therefore expect $b_C \approx B_J+0.25$ for objects with $B-V \approx 1.0$. Carter estimates the sky brightness on the Schmidt plate to have an uncertainty of 0.15 mag. Since the sky brightness on the AAT plate was inferred by comparison with the photometry on the Schmidt plate, the zero-point on the AAT plate has a slightly greater uncertainty.

Carter carried out the photometry of individual images, and the classification of stars and galaxies, using the methods of Carter & Godwin (1979). Any image that overlapped another at the 27 mag arcsec^{-2} isophote was tagged as being contaminated. The estimated random errors on the photometry from the AAT plate were 0.1 mag brighter than 20.5 mag, increasing to ~ 0.3 mag for the faintest images.

Carter's photometry was compared, galaxy by galaxy, with that obtained here by matching objects' positions. Fig. 2 plots b_C versus APM magnitude for all matched objects. The resulting relation is tight and linear at least as faint as $m_{APM}=8.5$ ($B_J \approx 20.5$). The points lying well off the main curve are all faint galaxies merged with brighter ones, which have been matched to the single merged image found by the APM. All these images were tagged by Carter as contaminated.

The best-fit line shown (solid line) was obtained by limiting the sample to objects brighter than $m_{APM}=8.5$ and performing repeated least-squares fitting followed by 3σ-clipping until a stable sample was achieved. This procedure prevented the false matches from figuring in the

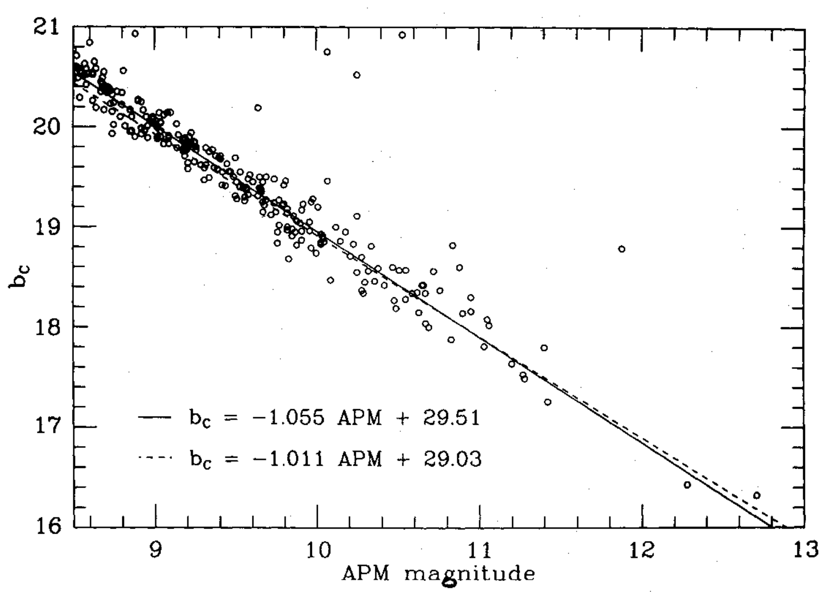

Figure 2. b_C (27.0 mag arcsec^{-2}) versus APM magnitudes for galaxies in the field of C03. The solid line is the best least-squares fit to the points with $m_{APM} \geq 8.5$ after 3σ-clipping to eliminate contaminated images (see text) until a stable sample is achieved. The dashed line is the CCD calibration for the same field (transformed from B_J to b_C).

best fit, which is $b_C = -1.055\, m_{APM} + 29.51$. The standard deviation about this fit (for objects with $m_{APM} \geq 8.5$) is 0.15 mag. Since the estimated random error in the Carter photometry is 0.1 mag, we can conclude that the random error in the APM magnitudes is also approximately 0.1 mag.

The dashed line in Fig. 2 is the CCD calibration for C03, transformed according to the expected relation $b_C \approx B_J + 0.25$. Nowhere over the range 9–13 in APM magnitude (approximately 16–20 in B_J) do the two calibrations differ by as much as 0.1 mag.

3 Analysis

3.1 DEFINITION OF SAMPLES

Lugger (1986) has stressed the importance of using homogeneous samples of galaxies when seeking to compare cluster LFs. Because the LF may vary with distance from the cluster centre, it is necessary to compare LFs constructed from galaxy samples with the same limiting radius if one is searching for variations due to other causes. It is likewise preferable to compare LFs over the same range of absolute magnitudes, especially when the comparison is made via model fits, as these can be misleading if their range of applicability is not specified.

Due to the factor of 3 in the range of redshifts in these clusters, it was not possible to realize the latter desideratum (a consistent faint absolute magnitude limit). The limit was instead chosen to be approximately the brighter of $B_J = 20$ and $m^* + 3$. For a cluster LF of Schechter (1976) form with characteristic apparent magnitude m^* and $\alpha = -1.25$, the galaxies brighter than $m^* + 3$ contain approximately 90 per cent of the total cluster galactic light, but fainter than $B_J = 20$ the number of objects rises rapidly, while the reliability of star/galaxy separation decreases. The exact magnitude limits employed are given in Table 2. In every case, however, the limiting radius for the galaxy sample was 1.5 h^{-1} Mpc (one Abell radius). This radius was chosen in order to allow comparison with most previous studies and to provide a reasonable signal-to-noise ratio in the LF over the range of redshift represented by the clusters.

All the images satisfying these limits on magnitude and radius were examined and classified by eye on the J survey film copies of the appropriate fields. The adopted visual classification system typed images as stars, galaxies, noise or merged galaxies. This last category, making up 11 per cent of all objects classed as galaxies, consisted of images which examination showed to be a galaxy merged with some other object. Of the galaxies with absolute magnitudes brighter than $M = -20$ (approximately M^*, the characteristic magnitude), 33 per cent are merged. (Note that unless specifically stated otherwise, M refers to absolute magnitudes in the B_J pass-band.) This increased fraction of merged objects is entirely due to the fact that brighter galaxies are usually also larger, but presents the problem that excluding merged objects from the LF samples will seriously, and disproportionately, deplete the bright end of the LF.

An examination of the 20 brightest objects in each of the 14 clusters showed that ~20 per cent were seriously (i.e. by more than 0.5 mag) contaminated by light from another galaxy or a star. Thus the inclusion of merged objects in the LF samples means that approximately 20 per cent of objects at the bright end of the LF will have significantly over-estimated magnitudes. The inclusion or exclusion of merged objects has little effect on the faint end of the LF, where they are considerably rarer. In order to ameliorate the effect of merged objects on the bright end of the LFs, the model fits and LF comparisons of the following sections ignore all objects brighter than $M = -21$. This limit also effectively excludes D and cD brightest cluster members, as is necessary when fitting a Schechter function to an LF (Schechter 1976).

Several previous studies of the cluster LF which have used photographic photometry (notably Oemler 1974 and Dressler 1978) make no mention of how the problem of merged images was dealt with, although similar problems must have been encountered. Lugger (1986) attempts a solution by estimating the magnitudes of overlapping images by eye and correcting accordingly, an approach whose reliability does not reward the pains taken. The photometric reduction of the Oxford group (e.g. Bucknell *et al.* 1979) apportions the light of merged images on a more sophisticated basis, but even so, as fig. 1 of Godwin & Peach (1977) shows, large errors from this source are still encountered. Any such scatter immediately translates into a bias of the LF towards brighter magnitudes, even if the introduced magnitude errors are themselves unbiased, since more galaxies are likely to be scattered into a magnitude bin from fainter magnitudes than from brighter magnitudes due to the steep increase of the LF towards fainter magnitudes.

Table 3, Microfiche MN 237/3, lists (in RA order) the positions and B_J magnitudes for all the objects in the 14 clusters that:

(i) are brighter than the limiting magnitudes given in column 5 of Table 2 [approximately $\min(20, m^*+3)$];
(ii) lie within 1.5 h^{-1} Mpc (an Abell radius) of the cluster centres given in Table 1;
(iii) were classified by eye to be either galaxies or merged galaxies.

3.2 CONSTRUCTION OF THE CLUSTER LFs

Construction of the differential LFs proceeds by first converting the observed apparent magnitudes of the galaxies to absolute magnitudes, using the measured redshift to give the distance modulus, and appropriate estimates of the K-correction and Galactic absorption. Next, the galaxies are binned by absolute magnitude in 0.5-mag bins, the limits of which lie at multiples of 0.5 mag. The expected number of field galaxies in each bin over the area of sky covered by the sample is then subtracted to give the field-corrected cluster differential LF. The details of this construction are given below.

To convert apparent magnitudes to absolute magnitudes the standard formula

$$M = m - \mu - A_J - K_z \qquad (4)$$

is used, where M is absolute magnitude, m is apparent magnitude, μ is the distance modulus, A_J is the galactic absorption (in the B_J pass-band) and K_Z is the K-correction. The distance modulus, μ, is given by

$$\mu = 42.384 - 5\log h + 5\log z, \qquad (5)$$

where we have assumed $q_0 = +1$ in accord with most other studies of cluster LFs (if not physical expectation). If we had assumed $q_0 = 0$ then the distance modulus would be increased by 0.05 mag at $z = 0.05$ and by 0.16 mag at $z = 0.15$. The inferred absolute magnitudes would be brighter by these amounts. The mean redshifts of the clusters are typically in error by 0.5 per cent, giving rise to negligible errors of ~ 0.01 mag in μ.

Corrections for interstellar absorption were made in accord with Burstein & Heiles (1982). They give $A_V = 3.3\,E(B-V)$ and $A_B = 4.3\,E(B-V)$, whence, by equation (2), $A_J = 4.0\,E(B-V)$. This relation, and values of $E(B-V)$ from fig. 6b of Burstein & Heiles were used to estimate A_J for each cluster. Only four clusters have non-zero absorption and in no case does absorption account for more than 0.2 mag. The patchiness of interstellar absorption makes the errors in A_J difficult to estimate, but they are probably no more than ~ 0.1 mag.

The K-corrections adopted here are those appropriate to E and S0 galaxies, computed from the tabulation by Shanks *et al.* (1984) of the polynomial fits of Ellis (1983) to calculated K-corrections in B_J, namely

$$K_z = 4.14z - 0.44z^2. \qquad (6)$$

This relation should approximate the K-correction to within 0.1 mag out to a redshift of 0.2. If the mix of galaxy types in a cluster were not dominated by E and S0 galaxies but instead had equal numbers of E's, S0's and spirals (as in Oemler's 1974 spiral-rich clusters), the mean K-correction at $z=0.05$ would decrease by ~ 0.05 mag and at $z=0.15$ decrease by ~ 0.15 mag. The inferred absolute magnitudes would be fainter by these amounts. These K-corrections should be in reasonable agreement with those of Oemler (1974) (who calculates K-corrections using the spectrum of the central galaxy in A2670), Dressler (1978) (who uses the K-corrections of Sandage 1973), Bucknell *et al.* (1979) (who use K-corrections based on those of Whitford 1971 and Schild & Oke 1971) and Lugger (1986) (who uses those of Persson, Frogel & Aaronson 1979). These latter are $K_z(V)=2z$ and $K_z(B-V)=3z$, which by equation (2) imply $K_z(B_J)=K_z(V)+0.72\,K_z(B-V)=4.16z$, in good agreement with equation (6) over the pertinent range of redshift.

3.3 FIELD GALAXY CORRECTIONS

Most previous studies of cluster LFs have adopted the galaxy counts made by Oemler (1974) and presented in his fig. 2. These field counts come from the outer parts of his cluster fields, supplemented at the bright end by counts from Zwicky *et al.*'s *Catalogue of Galaxies and Clusters of Galaxies* (1961–68). Oemler notes that, 'fluctuations in the number density of background galaxies are strong on all scales, but particularly at those corresponding to the clustering scale of objects at a particular distance'. Thus if one makes counts in the vicinity of a cluster one may well be biasing the background upwards because of superclustering. Conversely, making counts in regions subjectively chosen to be free of obvious clustering will tend to bias the background correction downwards.

Oemler found considerable scatter in his own counts and adopted a 50 per cent uncertainty in the background level. Dressler (1978) used Oemler's background correction and found that it agreed very well with his own background estimates made using the Shane–Wirtanen counts. His counts showed a standard deviation from field to field of 25 per cent, and he notes that this is consistent with the expected fluctuation in the angular covariance function for galaxies in the appropriate magnitude range over an angular size of 0°.5 and is considerably larger than a $\sqrt{N}$ fluctuation.

Several more recent sets of galaxy counts have been summarized in figs 2 and 6 of Ellis (1983). These various number counts, transformed (by Ellis) to B_J, are shown in Fig. 3 (crosses). Also shown is Oemler's (1974) mean relation (dotted curve), corrected to a bin size of 0.5 mag and transformed to B_J using $B_J = J - 0.11 + 0.41(J-F)$ (Ellis 1983) and $J-F=0.9$ (Oemler 1974) – i.e. $B_J = J + 0.26$. The agreement is remarkably good, although the curvature of the Oemler fit would not appear to be justified by these number counts.

A least-squares fit to the number counts from various sources given by Ellis (1983) is shown in Fig. 3 (solid line). The fit is

$$\log n_f = 0.502\,m - 7.57, \qquad (7)$$

where n_f is the number of galaxies per square degree per magnitude interval and m is the apparent B_J magnitude. This relation is adopted as the correction for field galaxies, and a field-to-field systematic error of 50 per cent assumed, following Oemler (1974) and Lugger (1986). That is to say that the error in the number of field galaxies in a given magnitude interval is taken to be

$$\delta N_f = \max(N_f^{1/2}, N_f/2), \qquad (8)$$

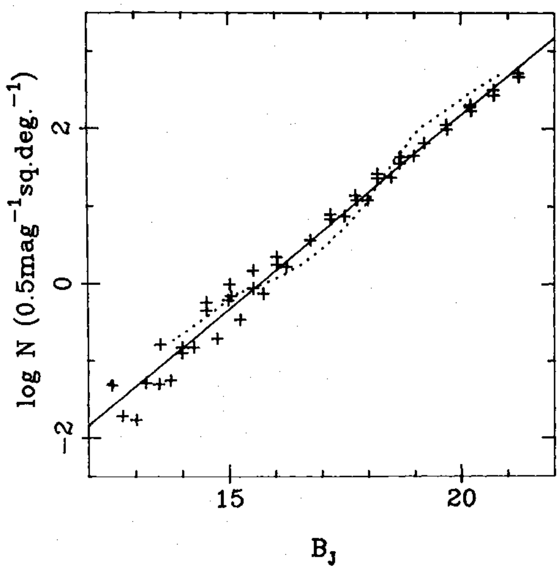

Figure 3. Field galaxy counts from Ellis (1983) shown as crosses (see text for sources), together with best least-squares fit (solid line). Also shown are the number counts (transformed to B_J and 0.5-mag bins) used by Oemler (1974) (dotted curve).

where N_f is the number of field galaxies expected in that magnitude interval. Note that although the field-to-field fluctuations in the number of field galaxies will cause systematic errors in the field-corrected LFs, equation (8) gives the appropriate error to use in applying χ^2 fits and comparisons to the data, since the χ^2 statistic takes no account of correlated deviations.

For each absolute magnitude bin of the differential LF the appropriate apparent magnitude at which to apply equation (7) for an estimate of the number of field galaxies is

$$m = M + \mu + K_z, \quad (9)$$

where M is the absolute magnitude of the bin centre. The absorption is *not* included in equation (9), since the number counts refer to high Galactic latitude fields, where zero absorption is assumed.

Errors in the field correction due to background fluctuations can have severe effects on the LFs of individual clusters, especially at the bright and faint ends where the number of galaxies in the cluster is comparable to the number in the field. For this reason the model fits and LF comparisons of the following sections ignore faint-end bins for which the number of cluster galaxies is less than either the expected number in the field or the number in the next-brightest bin. This procedure typically results in the LFs being fitted to a faint-end limit of $M \approx -18$.

3.4 SCHECHTER FUNCTION FITTING PROCEDURES

In fitting models to the observed LFs, the commonly-used Schechter function analytic approximation (Schechter 1976) is adopted. This choice facilitates comparison with previous LF studies, the majority of which have also adopted the Schechter model. The model is used here purely as an empirical fit that allows parameterization of the observed LFs, though it should be noted that it has the advantages over other common models (such as that suggested by Abell 1975) of having at least some theoretical justification (Press & Schechter 1974) and a small number of free parameters. In terms of absolute magnitude, the Schechter function model for the differential LF is

$$n_c(M)\,dM = kN^* \exp\{k(\alpha+1)(M^* - M) - \exp[k(M^* - M)]\}\,dM, \quad (10)$$

where M^* is the characteristic magnitude of the 'knee' of the LF, α is the exponent of the power law which the function asymptotes to at the faint end, and $k \equiv \ln(10)/2.5$.

This function was fitted to the field-corrected differential LFs by minimizing

$$\chi^2 = \sum_i \frac{(N_i - N_{ei})^2}{\sigma^2}, \tag{11}$$

where N_i is the number in the ith bin (centred on M_i) of the field-corrected LF; N_{ei} is the expected number from the Schechter function corrected for the finite bin width ΔM (Schechter 1976),

$$N_{ei} = n_c(M_i)\,\Delta M + n_c''(M_i)\,\Delta M^3/24, \tag{12}$$

and σ is the error in N_{ei}, taken to be

$$\sigma = [(N_{ei} + N_{fi}) + (\delta N_{fi})^2]^{1/2}. \tag{13}$$

$(N_{ei} + N_{fi})^{1/2}$ is the estimated Poisson error in the uncorrected LF. Following Lugger (1986), δN_{fi} is the error due to field-correction making allowance for systematic errors of ± 50 per cent,

$$\delta N_{fi} = \max(N_{fi}^{1/2}, N_{fi}/2), \tag{14}$$

in accord with equation (8).

The χ^2 statistic can be minimized with respect either to the parameters M^* and α, or to M^* alone, with α fixed. For individual clusters the errors in the LFs are such that only a single-parameter fit to M^* can be justified, and therefore α was fixed at -1.25, the value obtained by Schechter (1976) and Lugger (1986) when performing two-parameter fits to composite LFs formed from several clusters. (This choice is further justified in Section 3.6.) N^* was not taken as a free parameter, but was fixed by requiring that the total number of expected galaxies be equal to the total number in the field-corrected LF. The quoted error in M^* (when α is fixed) is the mean of the deviations from the best-fit value that increases χ^2 from $\chi^2_{\min}$ to $\chi^2_{\min} + 1$, and corresponds to the 68 per cent confidence interval.

A limitation of the χ^2-fitting technique is the loss of information involved in binning the individual data points. The method of maximum likelihood (ML) avoids this problem by dealing directly with the unbinned data. Moreover, the ML method is asymptotically unbiased and efficient, providing, for large samples, the most accurate and precise estimates possible for the parameters of the fitted model.

The ML estimates of the model parameters M^* and α (or M^* alone, with α fixed) are those values that maximize the log-likelihood function

$$\mathscr{L} = \sum_k \ln\left(\frac{n_c(M_k) + n_f(m_k)}{N_{tot}}\right), \tag{15}$$

where n_c is the differential cluster LF given by equation (10) and n_f is the differential field number–magnitude relation given by equation (7). M_k is the absolute magnitude of the kth galaxy in the sample, from which m_k is computed according to equation (9). The sum is over the entire sample of N_{tot} galaxies. As in the χ^2 fits, N^* ws not taken to be a free parameter, but was fixed by requiring that the total predicted and observed numbers of galaxies in the sample be equal.

Unlike the χ^2 fits, the ML method does not provide an intrinsic goodness-of-fit estimate. However, confidence intervals for the fitted parameters may be estimated using the fact that the log-likelihood ratio statistic $2[\mathscr{L}(\hat{\theta})-\mathscr{L}(\theta)]$, where θ is the vector of model parameters and $\hat{\theta}$ that vector which maximizes $\mathscr{L}$, is distributed approximately as χ^2_p, where p is the number of free parameters in the model (Dobson 1983). Thus when fitting M^* alone, the error quoted is the mean of the deviations from the ML estimate that give $\mathscr{L}=\mathscr{L}_{max}-0.5$ and corresponds to the 68 per cent confidence interval.

3.5 INDIVIDUAL CLUSTER LF PARAMETERS

Fig. 4 shows the differential LFs for each of the 14 clusters, together with their χ^2 best-fit $\alpha\equiv-1.25$ Schechter functions. The values for M^* obtained from the χ^2 fits and those obtained using the maximum likelihood method are summarized in Table 4. As inspection shows, the agreement between the two sets of fits is excellent: they lead to the same mean value of M^* and have an rms difference of 0.09 mag, indicating that no substantial amount of information is lost in binning the data.

The quantity $P(\chi^2|\nu)$ given in column 3 of the table is the confidence level at which the χ^2 fit can be rejected. With the given errors, the quality of the fits is generally good. Only C02 has a fit which may be rejected at the 5 per cent confidence level. Thus, accepting the error estimates used, an $\alpha\equiv-1.25$ Schechter function provides an adequate approximation to the form of the individual cluster LFs, with only a single possible counter-example amongst the 14 clusters.

The mean M^* for the 14 clusters is -20.12, and the standard deviation about this mean is 0.4 mag. Both values are in good agreement with previous results, some of which are summarized in Table 5 (where the original values of M^* have been transformed to B_J and $H_0=100$ km s^{-1}).

Dressler (1978) estimates the significance of variations of M^* about the mean, $\langle M^*\rangle$, by computing the standard deviation in estimates of M^* due to finite sample size, $\sigma(M^*)$, as a function of the number of galaxies in the cluster brighter than a given magnitude. Table 4 gives N_R, the field-corrected number of galaxies within 1.5 h^{-1} Mpc of the cluster centre (one Abell radius) that are brighter than $M=-19$ (i.e. brighter than about $\langle M^*\rangle+1$). Interpolating table 3 of Dressler (1978) to $\langle M^*\rangle+1$ and scaling according to $N^{-1/2}$ as he recommends, we obtain $\sigma(M^*)\approx 2/\sqrt{N_R}$. The ratio $\sigma=(M^*-\langle M^*\rangle)/\sigma(M^*)$ for the χ^2 fits is given in column 6 of Table 4.

On the basis of this test, only C37 and C39 show significant [i.e. $\sigma(M^*)\geq 3$] deviations of M^* from the mean. This latter cluster lies 40 arcmin (~ 1.5 h^{-1} Mpc) north of a much richer cluster (DC 2048 – 52) for which Dressler (1980a) obtains a redshift of 0.046. C39 is at $z=0.048$ (Paper I), and a contour map of the surface density of galaxies in the region (Geller & Beers 1982) shows a bridge of galaxies linking the two clusters. Of the 20 brightest objects in the LF sample, five lie in a tight group close to the centre of the cluster to the south, while a further six lie in another group 30 arcmin (~ 1 h^{-1} Mpc) to the west. The LF sample for C39 is thus to some extent confused by the presence of this second cluster.

In his own sample of 12 clusters, Dressler (1978) also found two clusters (A274 and A2029) with significant deviations from the mean M^*. Lugger (1986) found, similarly, a single significantly deviant value of M^* (for A569) in a sample of nine clusters. Since there are possible extrinsic causes for variations in M^* (such as contamination by fore- or background clusters and groups), as well as intrinsic ones, these results suggest that the great majority of clusters have LFs that are consistent (within the errors due to the finite sample sizes) with a common value of M^*. No more than about 15 per cent of clusters can have statistically significant intrinsic deviations of M^* from the value common to the remainder of the cluster population.

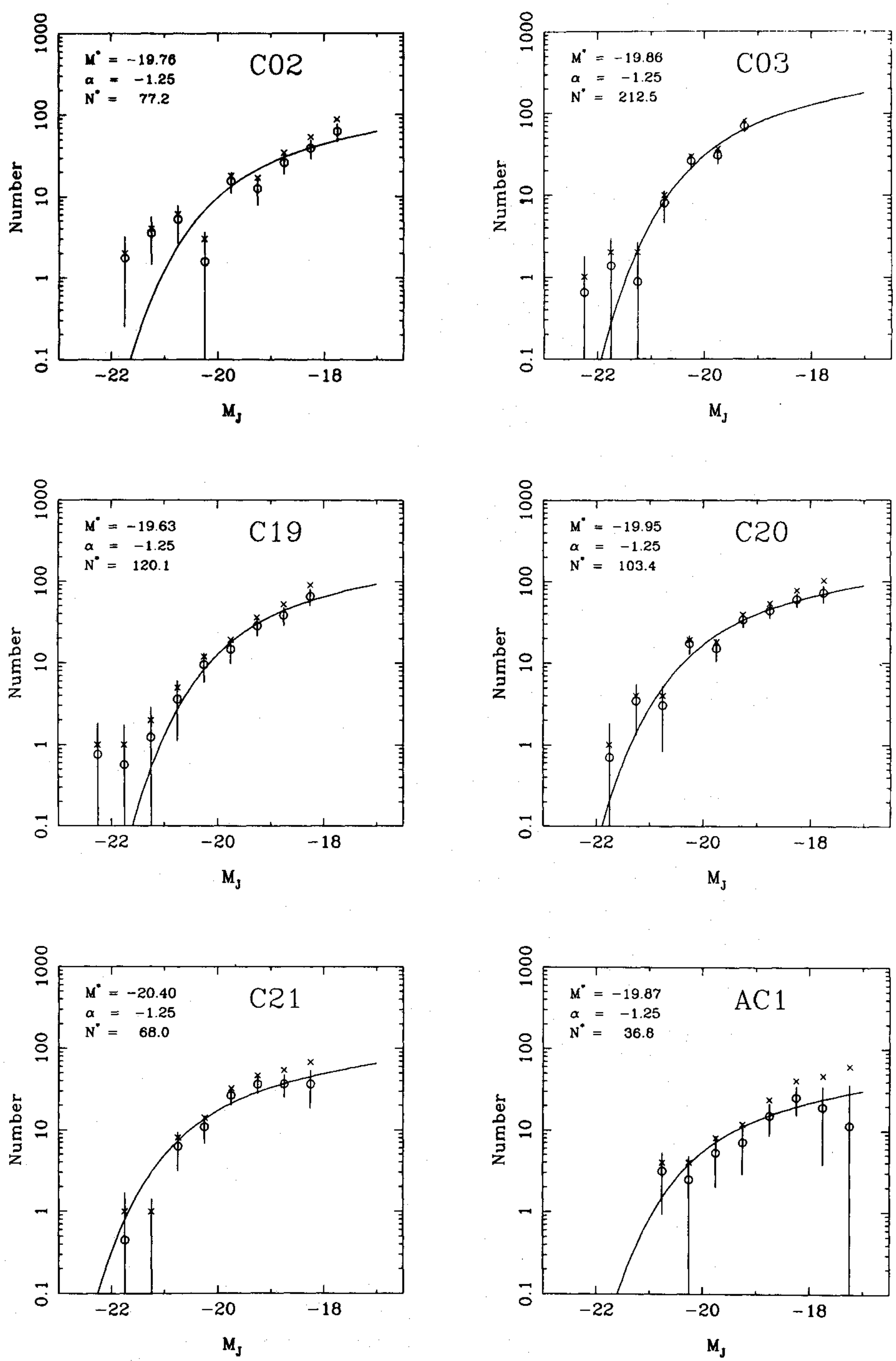

Figure 4. Field-corrected differential LFs for each cluster, with superimposed χ^2 best-fit $\alpha \equiv -1.25$ Schechter functions. Bins are 0.5 mag wide, crosses are raw counts, circles are field-corrected counts, error bars are as described in the text.

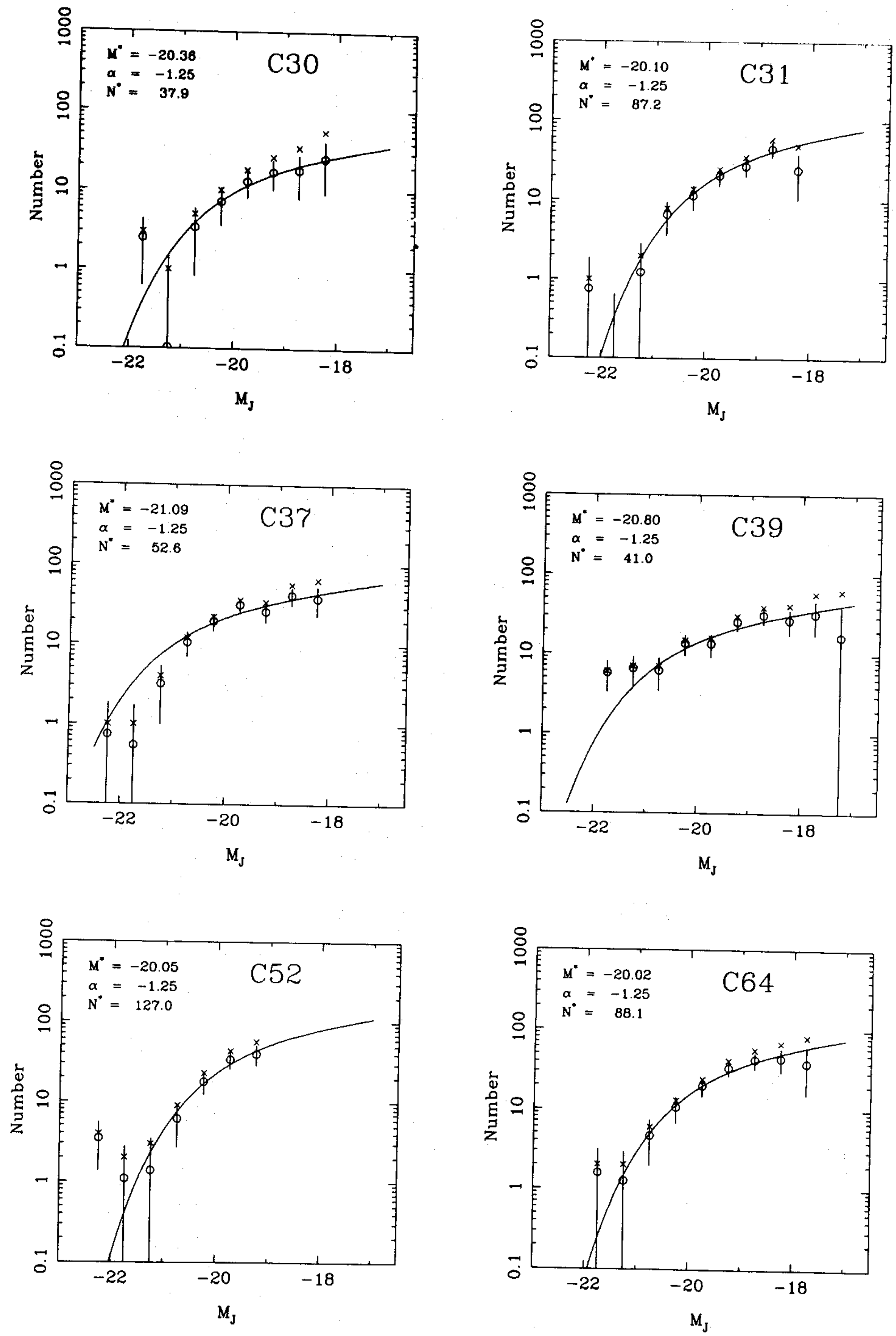

Figure 4 – *continued*

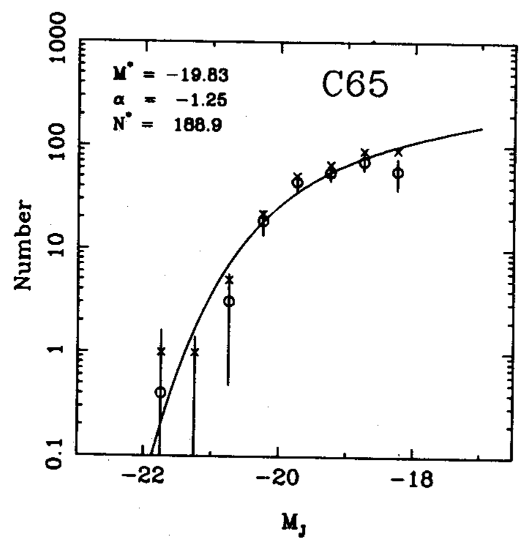

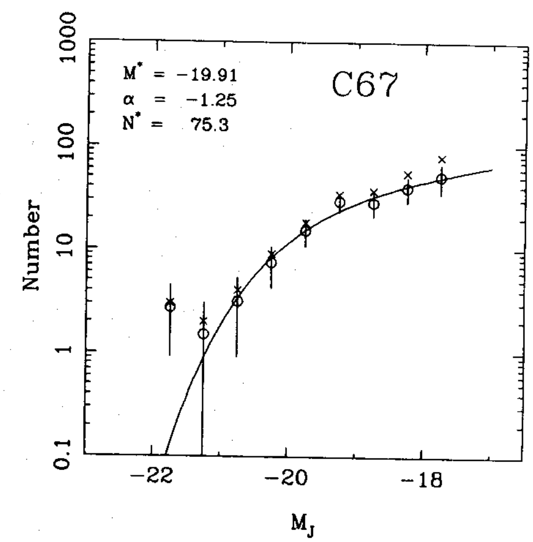

Figure 4 – *continued*

Table 4. Individual cluster LF parameters.

(1) Cluster	(2) M^* [(a)]	(3) $P(\chi^2\|\nu)$ [(b)]	(4) M^* [(c)]	(5) P_{KS} [(d)]	(6) N_R [(e)]	(7) σ [(f)]
C02	-19.76 (0.21)	0.02	-19.55 (0.25)	0.03	39.6	+1.1
C03	-19.86 (0.23)	0.06	-19.87 (0.23)	0.83	136.8	+1.5
C19	-19.63 (0.23)	0.56	-19.68 (0.23)	0.60	58.1	+1.9
C20	-19.95 (0.20)	0.31	-19.86 (0.19)	0.24	72.6	+0.7
C21	-20.40 (0.35)	0.27	-20.37 (0.32)	0.06	79.0	−1.3
AC1	-19.87 (0.46)	0.28	-19.79 (0.47)	0.30	16.7	+0.5
C30	-20.36 (0.58)	0.82	-20.45 (0.59)	0.06	42.1	−0.8
C31	-20.10 (0.30)	0.67	-20.19 (0.34)	0.70	67.2	+0.1
C37	-21.09 (0.41)	0.35	-21.10 (0.55)	0.0006	91.1	−4.7
C39	-20.80 (0.46)	0.56	-20.86 (0.48)	0.07	70.8	−2.9
C52	-20.05 (0.33)	0.32	-20.11 (0.32)	0.04	102.3	+0.4
C64	-20.02 (0.26)	0.78	-20.12 (0.27)	0.06	70.7	+0.4
C65	-19.83 (0.20)	0.10	-19.82 (0.19)	0.20	121.3	+1.6
C67	-19.91 (0.25)	0.81	-19.95 (0.25)	0.98	58.5	+0.8
Mean (s.d.)	-20.12 (0.41)		-20.12 (0.44)			

[(a)] Best χ^2 fit using $\alpha \equiv -1.25$ and excluding galaxies with $M < -21$.
[(b)] The confidence level at which the χ^2 fit may be rejected.
[(c)] Best ML fit using $\alpha \equiv -1.25$ and excluding galaxies with $M < -21$.
[(d)] The confidence level at which a one-sample KS test rejects the cluster as not being drawn from a Schechter LF with $M^* = -20.1$ and $\alpha = -1.25$.
[(e)] The field-corrected number of galaxies with $M < -19$ within 1.5 h^{-1} Mpc.
[(f)] σ is defined to be $(M^* - \langle M^* \rangle)/\sigma(M^*)$.

3.6 THE COMPOSITE LF

Composite LFs can be formed by combining the LFs of several clusters (or subsamples thereof) according to

$$N_{\rm cj} = \frac{N_{\rm c0}}{m_{\rm j}} \sum_i \frac{N_{\rm ij}}{N_{\rm i0}}, \qquad (16)$$

Table 5. Estimates of M^* and α for cluster and field LFs.

(1) Source	(2) Passband	(3) Comments	(4) M^* (s.d.)[a]	(5) α[b]
1. Schechter (1976)	J	Composite of 13 Oemler (1974) clusters	-19.9 (0.5)	-1.24
	$B(0)$	RCBG[c] (field)	-19.8	-1.24
2. Dressler (1978)	F	Mean of 12 clusters	-19.7 (0.5)	[-1.25]
3. Lugger (1986)	F	a. Mean of 9 clusters		
		(i) BCMs[d] included	-20.7 (0.6)	-1.47
			-20.2 (0.4)	[-1.25]
		(ii) BCMs excluded	-19.9 (0.6)	-1.24
			-19.8 (0.5)	[-1.25]
		b. Composite of 9 clusters		
		(i) BCMs included	-20.4	-1.39
		(ii) BCMs excluded	-19.9	-1.27
4. Kirschner *et al.* (1983)	J	Field	-19.9	[-1.25]

[a] Original values of M^* and α transformed to B_J and $H_0 = 100$ km s^{-1}.
[b] [− 1.25] ≡ fit to Schechter function made with this fixed α.
[c] RCGB ≡ *Reference Catalogue of Bright Galaxies.*
[d] BCM ≡ Brightest Cluster Member.

where N_{cj} is the number of galaxies in the jth bin of the composite LF, N_{ij} is the number in the jth bin of the ith cluster's LF, N_{i0} is the normalization of the ith cluster LF (taken here to be N_R, the field-corrected number of galaxies brighter than $M = -19$ within an Abell radius), m_j is the number of clusters contributing to the jth bin and

$$N_{c0} = \sum_i N_{i0}. \tag{17}$$

The formal errors of the composite LF are computed according to

$$\delta N_{cj} = \frac{N_{c0}}{m_j}\left[\sum_i \left(\frac{\delta N_{ij}}{N_{i0}}\right)^2\right]^{1/2}, \tag{18}$$

where δN_{cj} and δN_{ij} are the formal errors in the jth LF bin for the composite and the ith cluster, respectively.

A composite LF formed from all 14 clusters was constructed following the recipe outlined above. It is shown in Fig. 5(a) with the best χ^2 fit $(P(\chi^2|\nu)=0.91)$ to a two-parameter Schechter function on the range $-21 < M < -18$, which has $M^* = -20.04$ and $\alpha = -1.21$. (The magnitude range was chosen so that the fit would be directly comparable to the individual cluster fits.) These values are in excellent agreement with previous fits to composite LFs by Schechter (1976) and Lugger (1986) (see Table 5). The error contours of this fit are shown in Fig. 5(b). The fitted values of M^* and α are seen to be highly correlated, as noted by Schechter (1976). Almost as good a fit $[P(\chi^2|\nu) = 0.88]$ can be obtained keeping α fixed at -1.25, which case $M^* = -20.10\,(\pm 0.07)$ – see Fig. 5(c).

If we assume that the composite LF is a very good approximation to the hypothetical universal LF, we can make a non-parametric direct comparison of the individual cluster LFs to this supposed universal LF by a one-sample χ^2 test in which the expected distribution is taken to be the composite LF. χ^2 is calculated according to equation (11) with σ taken to be the

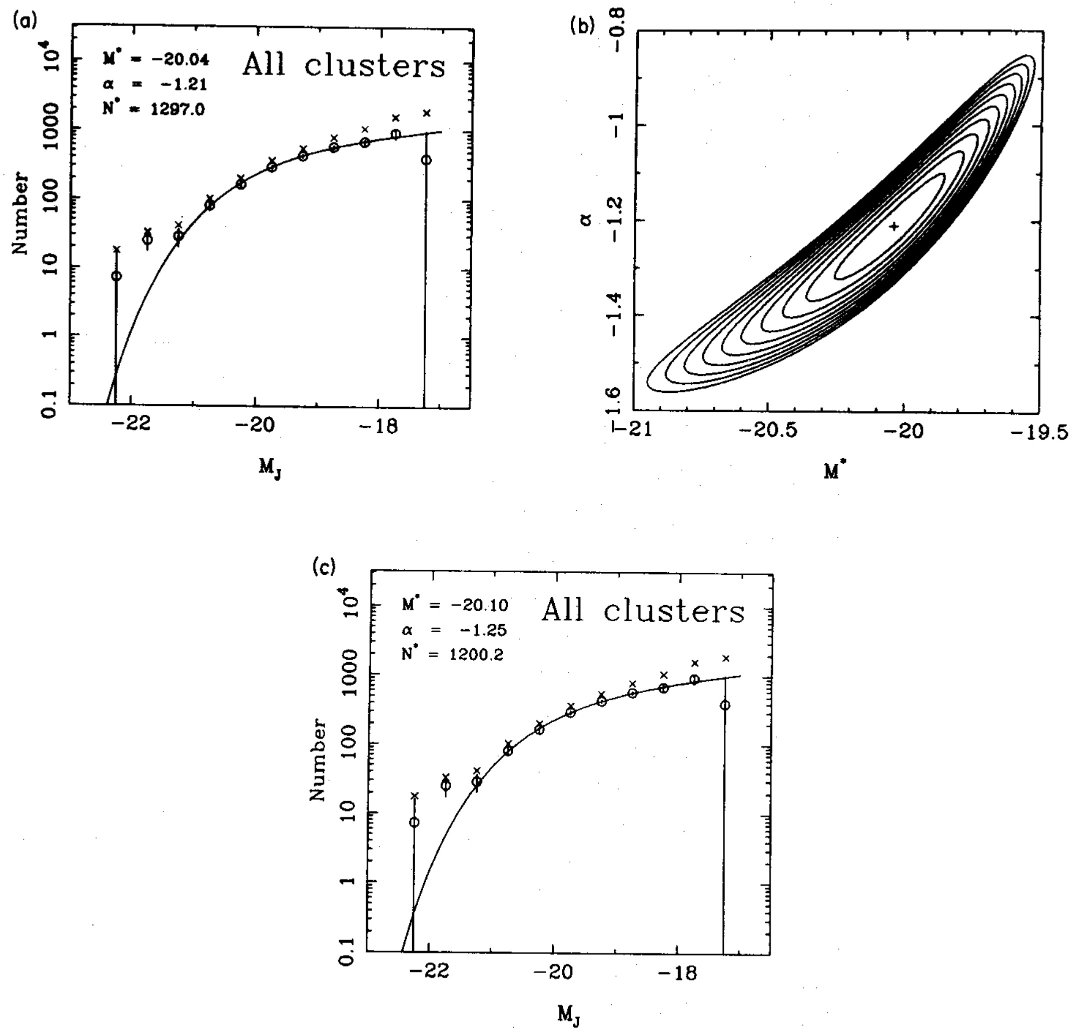

Figure 5. (a) The composite LF formed from all 14 clusters together with the best χ^2 two-parameter Schechter function fit; (b) the error contours for this fit; (c) the same as (a) except the fit is for α fixed at -1.25. In each case the fit is made to the range $-21 < M < -18$. Crosses are the uncorrected counts, circles the field-corrected counts, and error bars are as described in the text. The contour levels in the error plot are $\chi^2_{\min}+1, \ldots, \chi^2_{\min}+10$, with the cross marking the best fit. (NB the 68 per cent confidence ellipse corresponds to $\chi^2_{\min}+2.3$, 90 per cent to $\chi^2_{\min}+4.6$ and 99 per cent to $\chi^2_{\min}+9.2$ for normally-distributed errors.)

errors in the individual and composite LFs (equations 13 and 18) added in quadrature. As elsewhere, faint-end bins for which the number of cluster galaxies is less than either the expected number in the field or the number in the next-brightest bin are ignored, as are bins brighter than $M = -21$. Bright-end bins are summed together until five or more objects are expected in the brightest bin.

Under this test, no individual cluster LF differs from the composite at even the 10 per cent level. Lower limits on the error estimates, leading to the most stringent test of LF similarity, are obtained if σ is taken to be the square root of the expected number of objects in a bin ('Poisson errors'). Using these bare minimum error estimates, only C37 [with $P(\chi^2|\nu)=0.006$] can be rejected at better than the 10 per cent confidence level as not being drawn from a universal LF closely approximated by the composite. There is no reason to believe that any other cluster LF was not drawn from such a universal LF.

4 Discussion

4.1 IS THERE A UNIVERSAL LF?

To summarize the points made in the previous sections:

(i) χ^2 fits to the approximate range M^*-1 to M^*+2 show no evidence that the form of the great majority of individual cluster LFs cannot be adequately represented by a Schechter function with $\alpha \equiv -1.25$.

(ii) The mean characteristic magnitude, M^*, for the clusters in this study is in good agreement with the values obtained for both the field and cluster LFs in other studies (see Table 5). Thus both the form and the parameterization appear to be well-defined in the mean.

(iii) Comparison of the observed and expected values of $M^*-\langle M^*\rangle$ only identifies two of the 14 clusters as having characteristic magnitudes significantly ($\sigma \geq 3$) different from the mean of the sample. This fraction is consistent with the studies of Dressler (1978) and Lugger (1986), and suggests that no more than about 15 per cent of clusters can have values of M^* differing significantly from the value common to the bulk of the cluster population.

(iv) The composite LF formed from all 14 individual cluster LFs is best fitted by a Schechter function with $M^*=-20.04$ and $\alpha=-1.21$, and is also well-fit by a Schechter function with $M^*=-20.10$ and α fixed at -1.25. These results agree very well with previous fits to composite LFs by Schechter (1976) and Lugger (1986).

(v) Direct χ^2 comparison of each of the individual cluster LFs with the composite LF does not imply that any could not have been drawn from a universal LF represented by this composite. Re-applying the test using only $\sqrt{N}$ errors (surely an under-estimate) implies that at most one cluster could possibly not take on the universal form.

These several arguments force us to conclude that over the approximate magnitude range M^*-1 to M^*+2, the null hypothesis of a universal cluster LF of Schechter form and parameters $M^* \approx -20.1$, $\alpha \approx -1.25$ cannot be convincingly rejected.

As a further check on this result, we apply a Kolmogorov–Smirnov (KS) one-sample test to determine whether the distribution of observed galaxy magnitudes in each individual cluster could be drawn from a model distribution consisting of the assumed field contribution and a suitably normalized Schechter function with $M^*=-20.1$ and $\alpha=-1.25$. The magnitude range examined in each case was the same as that used in fitting the LFs.

The results are given in column 5 of Table 4. One cluster, C37, can be rejected at a confidence level of better than 1 per cent, and two others, C02 and C52, can be rejected at better than 5 per cent. These results are consistent with those obtained from the χ^2 comparison of the individual LFs with the composite LF using Poisson errors. As in that test, interpreting the KS confidence levels as rejecting the hypothetical cluster LF presumes that the adopted field count relation is correct, and thus may be too pessimistic in individual cases. For example, if the normalization of the field counts in C37 is reduced by 20 per cent, the confidence level at which the null hypothesis may be rejected is 2 per cent; if the normalization is reduced by 50 per cent, the confidence level of rejection is only 15 per cent.

How powerful are these tests in rejecting real variations in the clusters' LFs? A rough guide may be obtained by drawing a large number of Monte Carlo samples from a Schechter LF with parameters varying from the null hypothesis, and finding the probability with which the null hypothesis can be rejected by the one-sample KS test at the confidence level of interest. Fig. 6 shows the probability with which a sample drawn from a Schechter LF with either M^* or α differing from the hypothesized values of $M^*=-20$ and $\alpha=1.25$ can be rejected at the 5 per cent and 1 per cent confidence levels for various cluster richnesses (measured by N_R). In order

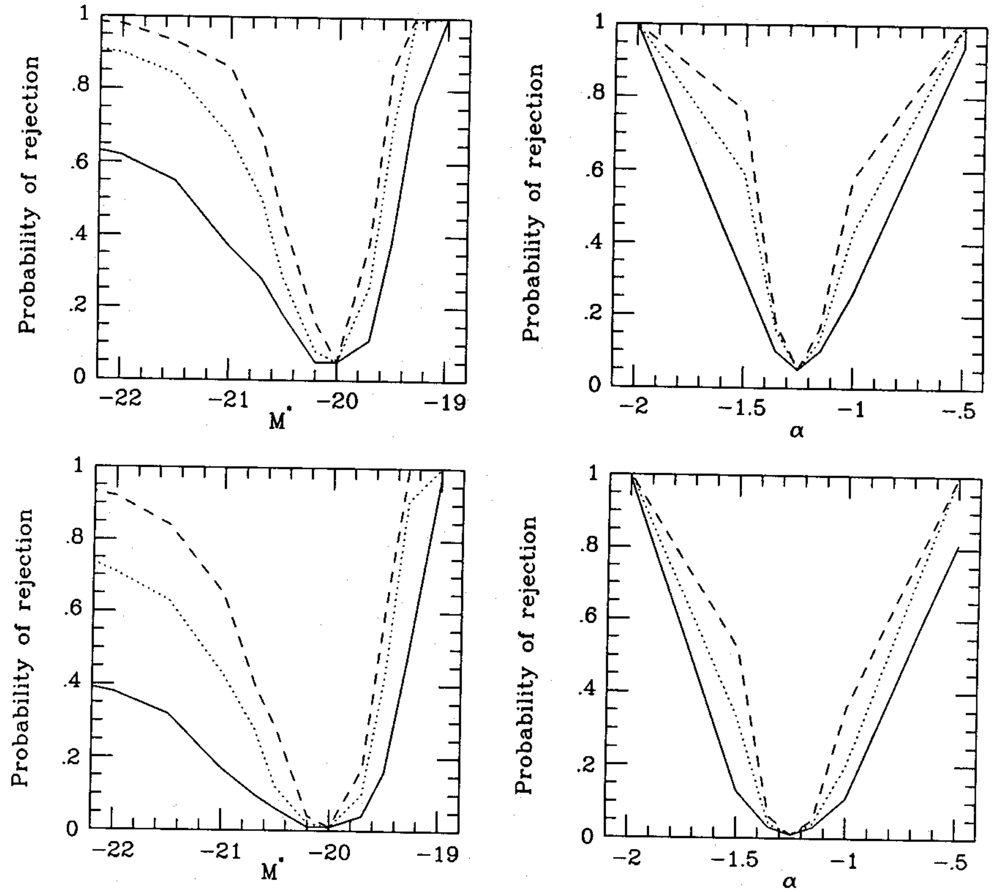

Figure 6. The power of a one-sample KS test to reject, as not being drawn from a Schechter function population with $M^* = -20$ and $\alpha = -1.25$, a sample drawn from a Schechter function with (on the left) M^* varying and $\alpha = -1.25$ or (on the right) α varying and $M^* = -20$. The top pair of panels are the rejection probability at the 5 per cent confidence level; the lower pair are for the 1 per cent confidence level. The solid line is for samples with $N_R = 40$; the dotted line, $N_R = 80$; the dashed line, $N_R = 120$.

to resemble as closely as possible the analysis carried out on the real data, the Monte Carlo samples were limited to the range $-21 \leq M \leq -18$.

Examination of Fig. 6 shows that the test is not always able to discriminate clearly against samples drawn from populations whose LF parameters differ from the parameters of the hypothesized population by amounts that would be considered physically meaningful and interesting (for example, a difference of 0.1 mag in M^*). In practice, other sources of error, such as the field-count normalization, make discrimination even more difficult. If we arbitrarily choose the level of 'effective' discrimination to be that at which a sample has a 50 per cent probability of being rejected at the 5 per cent confidence level, the figure shows that for $N_R = 40$, corresponding to the poorer clusters in the sample, the KS test is unable to discriminate effectively between $\alpha \equiv -1.25$ Schechter LFs with M^* in the range -21.2 to -19.4, or between $M^* \equiv -20$ Schechter LFs with α in the range -1.7 to -0.7. However, the situation is considerably better for the richer clusters in the sample: if $N_R = 120$ the corresponding undiscriminated ranges are -20.5 to -19.6 and -1.4 to -1.1.

Thus although we have no evidence for any variation of the individual cluster LFs from a Schechter LF with $M^* = -20.1$ and $\alpha = -1.25$, our tests are only able to rule out some of the physically meaningful variations in these parameters. Similarly, although the Schechter form for the LFs is certainly consistent with the data, other plausible forms for the LF cannot be rejected on the basis of such a test. This limited ability to discriminate genuine LF variations that would be of physical interest is *not*, however, a limitation due to the observational data or the analysis, but is a real property of the bright end of cluster LFs and a direct consequence of the small number of galaxies brighter than about M^*+2 in any individual cluster.

4.2 DO LFs VARY WITH CLUSTER PROPERTIES?

Several dynamical processes have the potential to change or determine the form of cluster LFs. Chief among these are: galaxy mergers, resulting from dynamical friction or direct collisions between galaxies; ram-pressure stripping of gas by the intracluster medium or during collisions; and tidal stripping of the outer parts of galaxies due to the mean cluster field or two-body interactions. The effects of some of these processes have been modelled in simulations of cluster evolution by Miller (1983), Merritt (1983, 1984, 1985) and Malumuth & Richstone (1984). We here briefly review the main conclusions reached in these studies.

In the galactic cannibalism picture of cD growth (Hausman & Ostriker 1978), Bautz–Morgan (B–M) type is a measure of the degree of cluster evolution, the main feature of which is depletion of the bright end of the LF as massive galaxies are consumed to form a cD. B–M types I and I-II would therefore be expected to have fewer bright galaxies than B–M type III, a trend that might be observed as fainter values of M^*.

Tidal stripping of galaxy haloes due to two-body interactions causes galaxies to become fainter. This effect is strongest for bright galaxies, leading to a depletion (or equivalently a steepening) of the bright end of the LF. Some simulations (Miller 1983) suggest that the faint end of the LF may be made flatter by this process. The efficiency of tidal stripping increases with increasing cluster density, so that one might expect fainter values of M^* and flatter faint-end slopes in clusters with higher central densities.

If post-collapse cluster evolution is small, whether because of tidal limitation of galaxies' haloes (as argued by Merritt 1984, 1985) or for other reasons, the shape of the cluster LF is established largely independently of the present-day cluster properties, so that little correlation between these properties and the form of the LF would exist.

All the simulations predict only insignificant amounts of luminosity segregation due to two-body interactions or dynamical friction, so that the LFs of the inner and outer parts of clusters should be indistinguishable.

In the light of these predictions, it is interesting to search for variations in cluster LFs correlated with richness, B–M type, velocity dispersion and distance from the cluster centre, both by comparison of characteristic magnitudes and by direct χ^2 tests. The results of the previous sections show that it is difficult to discriminate such variations in individual clusters. We therefore group clusters together on the basis of similar properties in order to reveal differences that are hidden by small-number statistics in individual cases. The groupings used are as follows:

(i) Richness: we compare the richest and poorest clusters, with richness measured by N_R, the field-corrected number of galaxies brighter than $M=-19$ within an Abell radius (see column 6 of Table 4). By this criterion the four richest clusters (having $N_R>90$) are C03, C37, C52 and C65 and the five poorest (having $N_R<60$) are C02, C19, AC1, C30 and C67.

(ii) B–M type: we compare the six clusters of B–M types I and I-II (C02, C03, C21, C30, C65, C67) with the five of type III (C19, C20, C31, C37, C39). The B–M types are as given in table 1 of Paper I, with C03 typed B–M following Carter (1980).

(iii) Velocity dispersion: we compare the clusters with $\sigma_v>1000$ km s^{-1} (C03, C19, C52) to those with $\sigma_v<700$ km s^{-1} (C02, C21, C30, C39). The line-of-sight velocity dispersions are from table 4 of Paper I. Note that AC1 is excluded from the former group as it is suspected to be two clusters projected along the line-of-sight, and so to have a spuriously high dispersion.

(iv) Distance from the cluster centre: we compare the LFs of the galaxies at distances R in the range $0<R<0.75\ h^{-1}$ Mpc with those having $0.75\ h^{-1}\ \mathrm{Mpc}<R<1.5\ h^{-1}$ Mpc for all clusters.

Table 6 summarizes these groupings and, for each except the last, gives the value of $\langle M^* \rangle$ and its standard error calculated from the χ^2 fits (with α fixed at -1.25) to individual cluster LFs. The values of $\langle M^* \rangle$ for two contrasted groupings differ by more than their joint error only in the case of high and low velocity dispersions, where the difference is 2.1 times the joint error, with the low dispersion clusters having the brighter value of M^*.

Figure 7 shows the composite LFs constructed for each of the above groupings along with their best-fit $\alpha \equiv -1.25$ Schechter functions. In order to avoid the problems caused by merged images at the bright end and by field subtraction at the faint end, and to better allow intercomparison, the fits were made uniformly to the range $-21<M<-18$ (see Sections 3.1 and 3.3). Table 7 lists the fit parameters and the associated confidence level for each LF.

Of the eight different groupings, only the composite LF of the high velocity dispersion clusters is significantly ill-fitted by an $\alpha \equiv -1.25$ Schechter function. The velocity dispersion pairing is likewise the only one with a difference in the fitted values of M^* greater than the joint

Table 6. Definitions of composite LFs.

(1) Composite LF	(2) Sample	(3) $\langle M^* \rangle$ (SEM)
0. All clusters	All 14 clusters	-20.12 (0.11)
1. Rich ($N_R>90$)	C03,C37,C52,C65	-20.25 (0.23)
2. Poor ($N_R<60$)	C02,C19,AC1,C30,C67	-19.91 (0.12)
3. B-M type I or I-II[a]	C02,C03,C21,C30,C65,C67	-20.05 (0.14)
4. B-M type III	C19,C20,C31,C37,C39	-20.31 (0.27)
5. High σ_v ($\sigma_v>1000\ km\ s^{-1}$)	C03,C19,C52	-19.85 (0.09)
6. Low σ_v ($\sigma_v<700\ km\ s^{-1}$)	C02,C21,C30,C39	-20.33 (0.21)
7. Inner region ($0<R<0.75h^{-1}Mpc$)	All 14 clusters	–
8. Outer region ($0.75h^{-1}Mpc<R<1.5h^{-1}Mpc$)	All 14 clusters	–

[a]C03 is taken to be B–M I (Carter 1980) although classified B–M II in the SCS.

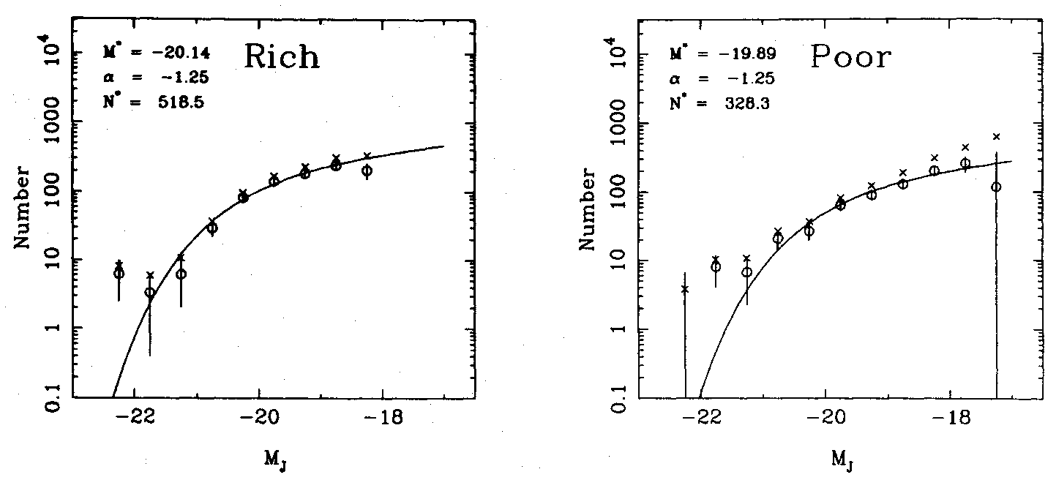

Figure 7. The composite LFs defined in Table 7 and their χ^2 best-fit Schechter functions for $\alpha \equiv -1.25$. The fits are made uniformly to the range $-21<M<-18$. Crosses are the uncorrected counts, circles the field-corrected counts and error bars are as described in the text.

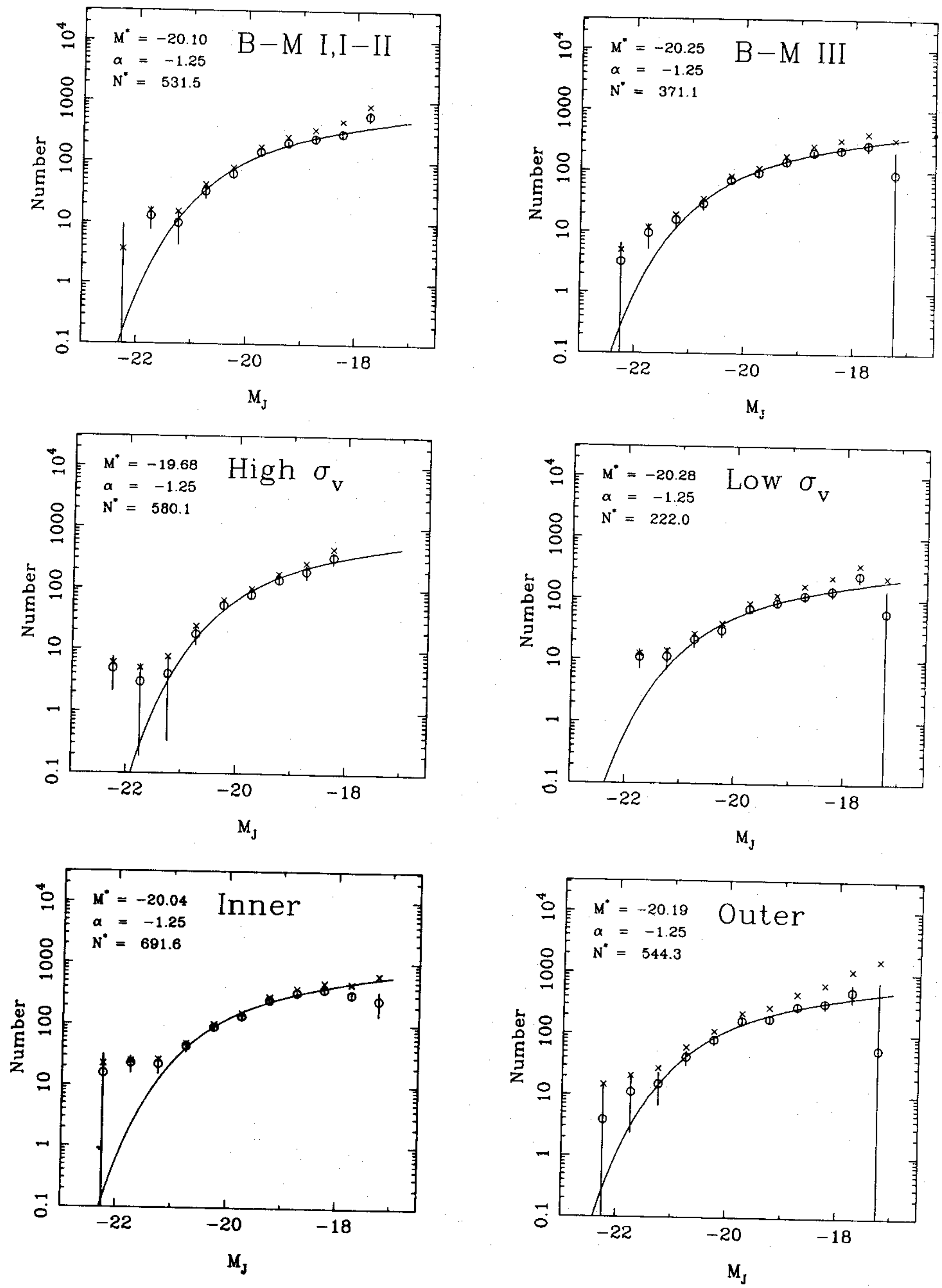

Figure 7 – *continued*

error. The sense of this difference is that the composite LF of the high velocity dispersion clusters has a fainter value of M^* than that of the low velocity dispersion clusters, corresponding to a steeper bright-end slope.

In order to directly test whether the pairs of composite LFs belonging to contrasted groupings could both have been drawn from the same underlying distribution (i.e. whether the LFs are statistically equivalent), we apply a two-sample χ^2 test assuming errors computed via

Table 7. Fits to composite LFs.

(1) Composite LF[a]	(2) M^* [b]	(3) $P(\chi^2 \mid \nu)$[c]
0. All	-20.10 (0.07)	0.88
1. Rich	-20.14 (0.11)	0.25
2. Poor	-19.89 (0.13)	0.07
3. Early B-M type	-20.10 (0.11)	0.12
4. Late B-M type	-20.25 (0.13)	0.44
5. High σ_v	-19.68 (0.09)	0.01
6. Low σ_v	-20.28 (0.18)	0.54
7. Inner region	-20.04 (0.09)	0.11
8. Outer region	-20.19 (0.12)	0.11

[a] Defined in Table 7.
[b] Fitted to $-21 \le M \le -18$ using $\alpha \equiv -1.25$.
[c] The confidence level at which the χ^2 fit may be excluded.

equation (18). The results of such tests show that no pair of LFs can be considered dissimilar at even a 10 per cent confidence level. As previously, we provide a check on the security of this conclusion against overestimates of the errors in the LFs by re-applying the test assuming 'Poisson' errors (certainly an underestimate). Even under this assumption, the rich and poor pairing and the B–M types I and I-II and B–M type III pairing show no significant differences. The inner region LF differs from the outer region LF at the 2 per cent confidence level, while the high and low velocity dispersion LFs differ at a level better than 1 per cent. Of the various properties examined, therefore, only velocity dispersion can be marginally associated with a variation in the cluster LF.

Because the form of the field contribution differs from one composite LF to another, intercomparison must be between the field-corrected LFs using the two-sample χ^2 test rather than directly between the combined magnitude distributions (inclusive of the field) using the equivalent KS test. It is, however, instructive to use the two-sample KS test as a guide in estimating the level at which variations between the composite LFs could be discriminated. Fig. 8 shows the probability with which variations in M^* and α can be rejected using a two-sample KS test, for a range of sample sizes. For the sake of example, both samples in the test are assumed to be of the same size. One is assumed to be drawn from a population with $M^* = -20$ and $\alpha = -1.25$, and the other from a population with either M^* or α varying from these values.

For the composite LFs constructed here, the typical value of N_R is 300. From Fig. 8 it can be seen that for this sample size the level of 'effective' discrimination (as before, the variation which gives the samples a 50 per cent probability of being found different at the 5 per cent confidence level) is $\Delta M^* = \pm 0.4$ mag or $\Delta\alpha = \pm 0.15$. Variations of either parameter alone by more than these amounts should be detected, though because M^* and α are highly correlated, joint variations may be larger. Examination of the differences in M^* displayed by the contrasted composite LFs in Table 6 or 7 would suggest that the high and low velocity dispersion pairing should be (marginally) effectively discriminated, in agreement with the result of the two-sample χ^2 test above.

One important source of possible LF differences, which has not been addressed here, is that associated with cluster-to-cluster variations in the mix of galaxy morphological types (see Dressler 1980b). What differences in cluster LFs might we expect from different morpho-

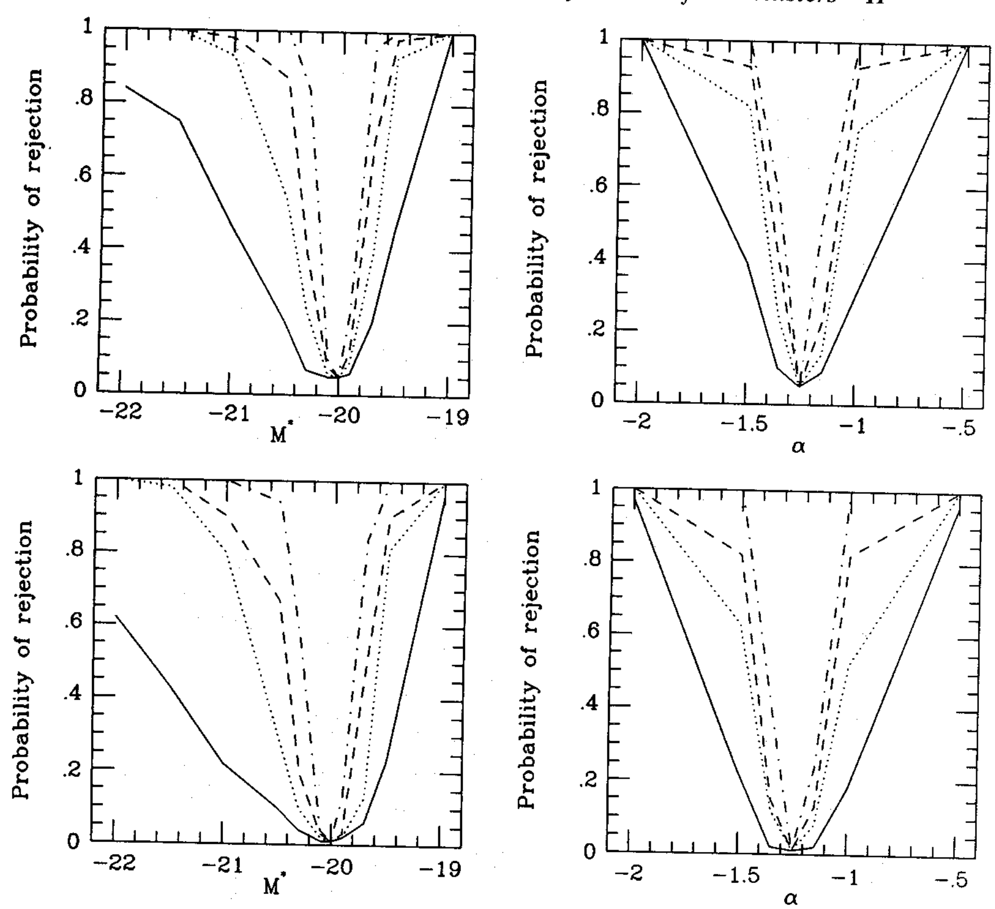

Figure 8. The power of a two-sample KS test to reject, as not being drawn from the same population, two samples of equal size, one drawn from a Schechter function with $M^* = -20$ and $\alpha = -1.25$ and the other drawn from a Schechter function with either (on the left) M^* varying and $\alpha = -1.25$, or (on the right) α varying and $M^* = -20$. The top pair of panels are the rejection probability at the 5 per cent confidence level; the lower pair are for the 1 per cent confidence level. The solid line is for samples each with $N_R = 100$; the dotted line, $N_R = 300$; the dashed line, $N_R = 500$; the dot–dash line, $N_R = 1000$.

logical mixes? Would these be detectable by the methods and sample sizes used here? The first question may be answered by reference to the work of Thompson & Gregory (1980), who used their LFs for ellipticals and lenticulars in Coma, and the field spiral LF of Christensen (1975), to synthesize LFs with the range of mixes of these galaxy types found in Dressler's (1980b) survey. The resultant LFs had a variation in M^* of ~ 0.5 mag. This is in fact the dispersion in M^* that is observed between individual clusters here.

Fig. 8(a) shows the LFs for the various galaxy types used by Thompson & Gregory (1980), while Fig. 8(b) shows the cluster LFs obtained by combining the individual types in the proportions given by Oemler (1974) as typical of his cD, spiral-poor and spiral-rich clusters. The differences are clearly small. The most extreme variation in the LF that is allowable, given the range of mixes observed by Dressler (1980b) is shown in Fig. 8(c). The difference between these LFs is no greater than that between the high and low velocity dispersion composite cluster LFs shown in Fig. 5, which could not be shown to be more than marginally significant.

With the possible exception of cluster velocity dispersion, none of the cluster properties considered here are associated with detectable LF variations greater than about 0.4 mag in M^* or 0.15 in α. Smaller variations are, however, possible. Detecting a variation of ~ 0.2 mag in M^* or ~ 0.1 in α, such as might be expected from different morphological mixes, would require a factor of 4 or more increase in sample size (*cf.* Fig. 8). A similar increase is probably

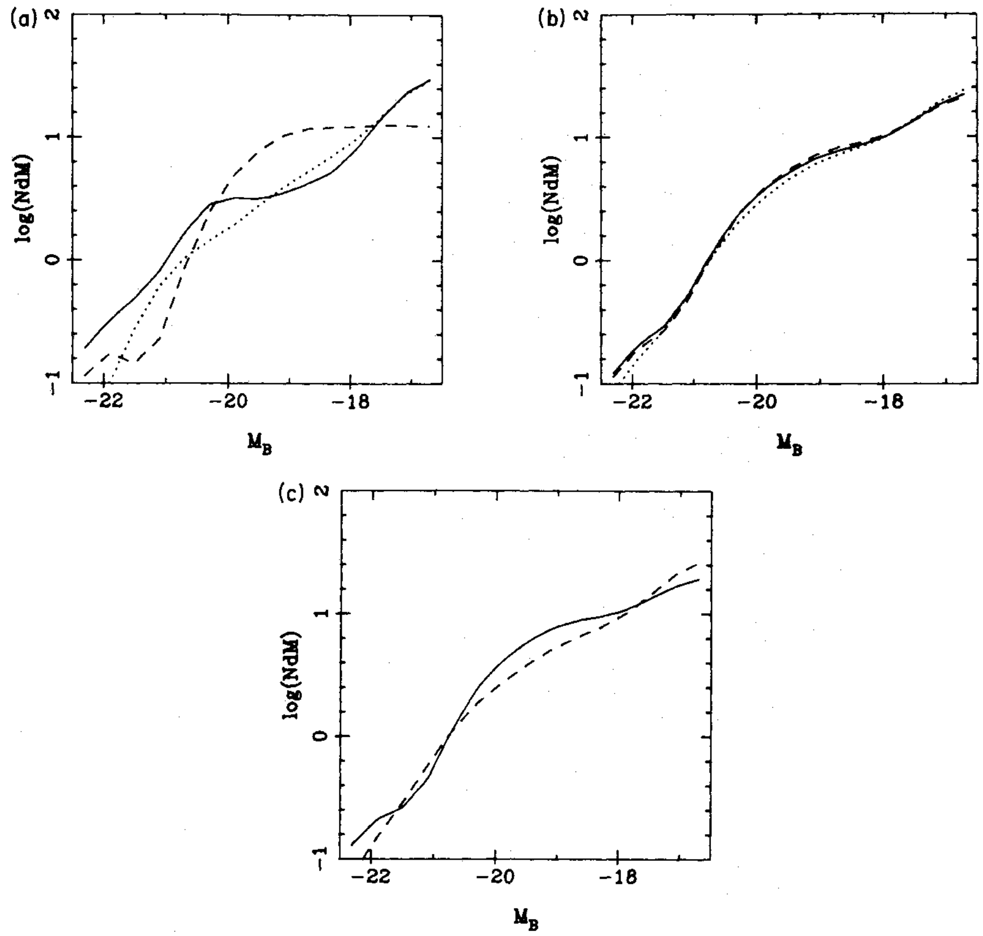

Figure 9. (a) LFs for ellipticals, lenticulars and spirals (solid, dashed and dotted lines, respectively) from Thompson & Gregory (1980); (b) these LFs combined in the ratios (E:S0:Sp) typical of Oemler's (1974) cD (3:4:2, solid line), spiral-poor (1:2:1, dashes) and spiral-rich (1:2:3, dots) clusters; (c) the extreme LFs allowed given Dressler's (1980b) range of morphological mixes (1:1:3, solid, and 3:6:1, dashes).

also required in order to detect differences in cluster LFs that may be caused by dynamical evolution, although the nature and amplitude of any such variations are still not well established by the simulations.

5 Conclusions

We have examined the LFs of 14 rich clusters and found them to be well-fitted, within the errors, by Schechter functions with $\alpha \equiv -1.25$. The mean M^* from both χ^2 and maximum likelihood fits is -20.12 (in the B_J pass-band) and the dispersion about this mean is 0.4 mag, both of which values are in good agreement with those derived in other studies of cluster LFs. A composite LF formed from all 14 clusters was found to be very well fitted by a Schechter function with $M^* = -20.04$ and $\alpha = -1.21$ over the range $-21 \leq M \leq -18$, and almost equally well fitted by a Schechter function with α fixed at -1.25 and $M^* = -20.10$.

Comparison of the fitted values of M^* using the method of Dressler (1978) suggested that two clusters, C37 and C39, may have characteristic magnitudes differing significantly from the mean. A one-sample χ^2-test, however, was unable to reject any cluster as not being drawn from a hypothetical universal LF assumed to be closely approximated by the composite LF of all 14 clusters. Under the very stringent assumption that the adopted number–magnitude relation for the field is correct, this same test only rejected C37 at better than the 1 per cent confidence level. With the same assumption, a one-sample Kolmogorov–Smirnov test to determine if the individual cluster LFs could have been drawn from a universal LF of Schechter form with $M^* = -20.1$ and $\alpha = -1.25$ also rejected only C37 at the 1 per cent level. If the estimated contribution to the LF from the field for this cluster were over-estimated by 25 per cent, consistent with the field-to-field variations noted by Dressler (1978), the confidence level at which this latter test rejects C37 drops to 2 per cent.

With the possible exception of C37, this analysis did not identify any cluster as a convincing counterexample to the null hypothesis of a universal LF of approximately Schechter form and parameters $M^* \approx -20.1$ and $\alpha \approx -1.25$. It must be noted that this conclusion only applies to the magnitude range covered by this study, approximately M^*-1 to M^*+2. Moreover, simulations show that it is statistically difficult to discriminate variations in the bright end of the LF due to the small number of galaxies brighter than M^*+2 in any individual cluster. The statistical consistency of the bright end of the observed cluster LFs with a universal LF thus does not rule out small but physically interesting variations in the underlying populations.

Guided by recent simulations of cluster evolution that provide predictions for the effect of the major dynamical processes on the form of cluster LFs, variations in the LFs correlated with cluster richness, B–M type and velocity dispersion were sought. The possibility that the LF may differ between the cluster centre and the periphery due to mass segregation induced by dynamical friction or two-body interactions was also considered. Mindful of the difficulty in discriminating between LFs having only a small number of galaxies, differences between the contrasted properties were sought by comparing composite LFs representing the richest and poorest clusters, B–M types I and I-II and B–M type III, inner regions and outer regions, and high and low velocity dispersions, in order to discover whether the contrasted LFs could not both have been drawn from the same underlying LF.

A two-sample χ^2-test showed that in no case could this hypothesis be rejected, although the composite LF of the high dispersion clusters could possibly have differed from that of the low velocity dispersion clusters if the errors in the LFs had been slightly overestimated. This marginal difference between the two composite LFs takes the form of a steeper bright end in the LF of the high velocity dispersion clusters, manifesting itself as a fainter mean characteristic magnitude for this group of clusters. A similar comparison of the composite LFs of the inner and outer regions of all 14 clusters showed no evidence for any mass segregation in the clusters.

Using simulations to estimate the power of the statistical tests, it is found that variations between the composite LFs of more than about 0.4 mag in M^* or 0.15 in α can be ruled out. However, detecting differences as small as 0.2 mag in M^* or 0.1 in α, such as would be expected from variations in the morphological mix from cluster to cluster, or the effects of dynamical evolution, would require the comparison of composite LFs with $N_R > 1000$.

Acknowledgments

I thank the APM group at Cambridge for guidance in using their measuring machine. Steve Maddox carried out the APM scans. Telescope time at CTIO (funded by AURA Inc.) is gratefully acknowledged. Paul Hewett, George Efstathiou, John Lucey, Richard Ellis and the anonymous referee provided useful comments and criticisms. The work was carried out at the Institute of Astronomy, Cambridge, with the support of a Shell Australia Science and Engineering Scholarship, and at the Department of Physics, University of Durham, with the support of a SERC PDRA. All computing was performed on the Cambridge and Durham nodes of STARLINK.

References

Abell, G. O., 1958. *Astrophys. J. Suppl.,* **3,** 211.

Abell, G. O., 1975. In: *Stars and Stellar Systems IX: Galaxies and the Universe,* p. 601, eds Sandage, A., Sandage, M. & Kristian, J., University of Chicago, Chicago.

Abell, G. O. & Corwin, H. G., 1983. In: *Early Evolution of the Universe and its Present Structure, IAU Symp. No. 104,* p. 179, eds Abell, G. O. & Chincarini, G., Reidel, Dordrecht.

Adams, M., Christian, C., Mould, J., Stryker, L. & Tody, D., 1980. *Stellar Magnitudes from Digital Pictures,* p. 1, KPNO, Tucson.

Blair, M. & Gilmore, G., 1982. *Publs astr. Soc. Pacif.,* **94,** 741.

Bucknell, M. J., Godwin, J. G. & Peach, J. V., 1979. *Mon. Not. R. astr. Soc.,* **188,** 579.

Burstein, D. & Heiles, C., 1982. *Astr. J.,* **87,** 1165.

Cannon, R. D., Hawarden, T. G., Sim, M. E. & Tritton, S. B., 1978. *Occ. Rep. R. Obs. Edinburgh,* No. 4.

Carter, D., 1980. *Mon. Not. R. astr. Soc.,* **190,** 307.

Carter, D. & Godwin, J. G., 1979. *Mon. Not. R. astr. Soc.,* **187,** 711.

Christensen, C. G., 1975. *Astr. J.,* **80,** 282.

Colless, M. & Hewett, P., 1987. *Mon. Not. R. astr. Soc.,* **224,** 453 (Paper I).

Dobson, A. J., 1983. *An Introduction to Statistical Modelling,* p. 40, Chapman and Hall, London.

Dressler, A., 1978. *Astrophys. J.,* **223,** 765.

Dressler, A., 1980a. *Astrophys. J. Suppl.,* **42,** 565.

Dressler, A., 1980b. *Astrophys. J.,* **236,** 351.

Ellis, R. S., 1983. In: *The Origin and Evolution of Galaxies,* p. 225, eds Jones, B. J. T. & Jones, J. E., Reidel, Dordrecht.

Geller, M. J. & Beers, T. C., 1982. *Publs astr. Soc. Pacif.,* **94,** 421.

Godwin, J. G., 1976. *PhD thesis,* University of Oxford.

Godwin, J. G. & Peach, J. V., 1977. *Mon. Not. R. astr. Soc.,* **181,** 323.

Green, M. R. & Dixon, K. L., 1978. *Observatory,* **98,** 166.

Hausman, M. A. & Ostriker, J. P., 1978. *Astrophys. J.,* **224,** 320.

Irwin, M. J. & Trimble, V., 1984. *Astr. J.,* **89,** 83.

Kibblewhite, E. J., Bridgeland, M. T., Bunclark, P. & Irwin, M. J., 1983. In: *Proceedings of the Astronomy Microdensitometry Conference,* ed. Klinger Smith, D., III (AMC).

Kirschner, R. P., Oemler, A., Schechter, P. L. & Schectman, S. A., 1983. *Astr. J.,* **88,** 1285.

Kron, R., 1980. *Astrophys. J. Suppl.,* **43,** 305.

Landolt, A. U., 1983. *Astr. J.,* **88,** 439.

Lugger, P., 1986. *Astrophys. J.,* **303,** 535.

Malumuth, E. & Richstone, D. O., 1984. *Astrophys. J.,* **276,** 413.

Merritt, D., 1983. *Astrophys. J.,* **264,** 24.

Merritt, D., 1984. *Astrophys. J.,* **276,** 26.

Merritt, D., 1985. *Astrophys. J.,* **289,** 18.

Miller, G. E., 1983. *Astrophys. J.,* **268,** 495.

Oemler, A., 1974. *Astrophys. J.,* **194,** 1.

Persson, S. E., Frogel, J. A. & Aaronson, M., 1979. *Astrophys. J. Suppl.,* **39,** 61.

Press, W. H. & Schechter, P., 1974. *Astrophys. J.,* **187,** 425.

Rainey, G. W., 1977. *PhD thesis,* University of California at Los Angeles.

Sandage, A., 1973. *Astrophys. J.,* **183,** 711.

Schechter, P. L., 1976. *Astrophys. J.,* **203,** 297.

Schild, R. & Oke, J. B., 1971. *Astrophys. J.,* **169,** 209.

Shanks, T., Stevenson, P. R. F., Fong, R. & MacGillivray, H. T., 1984. *Mon. Not. R. astr. Soc.,* **206,** 767.

Thompson, L. A. & Gregory, S. A., 1980. *Astrophys. J.,* **242,** 1.

Tody, D., 1986. *Proc. Soc. photo-opt. Instr. Eng.,* **627,** 733.

Whitford, A. E., 1971. *Astrophys. J.,* **169,** 215.

Zwicky, F., Herzog, E., Wild, P., Karpowicz, M. & Kowal, C. T., 1961–68. *Catalogue of Galaxies and Clusters of Galaxies,* Vols 1–6, Caltech, Pasadena.